1

Modeling (Visco)elasticity of Macromolecular and Biomacromolecular Networks

Fanlong Meng[1,2,3]

[1] *Chinese Academy of Sciences, CAS Key Laboratory for Theoretical Physics, Institute of Theoretical Physics, Beijing 100190, China*
[2] *University of Chinese Academy of Sciences, School of Physical Sciences, Beijing 100049, China*
[3] *University of Chinese Academy of Sciences, Wenzhou Institute, Wenzhou 325000, China*

When polymers are permanently crosslinked into a network, e.g., by covalent bonds which possess a very high energy barrier to break, then the network is elastic and can sustain mechanical loadings, resulting from the conformational entropy of the polymers if not considering other specific intramolecular/intermolecular interactions. By replacing the permanent crosslinks with the transient ones (low energy barriers to break and/or re-form), which can be either physical crosslinks formed by physical interactions (hydrogen bonds, guest-host interactions, hydrophobicity, etc.) or chemical ones whose breakage energy barrier is low (e.g., by adding catalysts), then the crosslinked network can dynamically re-organize its topological structure by the crosslink breakage/re-formation; the network can be treated as complex fluids, exhibiting interesting viscoelastic properties. Due to their characteristic rheological properties, the products made of the macromolecular networks (both permanently and transiently crosslinked ones) are widely utilised in various applications such as rubber bands, tires, self-healing materials, etc. As a special class of the macromolecular networks, the biomacromolecular networks are ubiquitous in nature such as cytoskeletons and extracellular matrices, which are relevant with various bio-functions including shape maintenance of cells, cell division, and movements. In the following, we will introduce the well-known theories of permanent macromolecular networks consisting of flexible polymers in Section 1.1 and those of permanent biomacromolecular networks consisting of semiflexible polymers in Section 1.2, discuss the viscoelastic responses of transient macromolecular networks in Section 1.3, and then finish this chapter with a brief discussion about some possible developments in the future.

Dynamics and Transport in Macromolecular Networks: Theory, Modeling, and Experiments,
First Edition. Edited by Li-Tang Yan.

1.1 Permanent Macromolecular Networks

As polymers are the main entity of the macromolecular network, the physical properties of *a single polymer* are very important in determining the overall responses of the network.

1.1.1 Mechanic Properties of a Single Polymer Chain

For a single polymer, one can define a *persistence length* [1, 2] to quantify the bending rigidity of the polymer ($l_\mathrm{p} = \kappa/k_\mathrm{B}T$, with κ as the bending rigidity, k_B as the Boltzmann constant, and T as the temperature), over which the correlations in the tangent direction along the polymer are lost. A relevant physical quantity is *Kuhn length* [1], which is $l_\mathrm{k} = 2l_\mathrm{p}$, over which the polymer can be treated as freely joint. By comparing the contour length l_c and persistence length l_p (as shown in Figure 1.1), polymers can be categorized into flexible ($l_\mathrm{c} \gg l_\mathrm{p}$), semiflexible ($l_\mathrm{c} \simeq l_\mathrm{p}$) and rigid ($l_\mathrm{c} \ll l_\mathrm{p}$) ones. Usually, synthetic polymers such as polyethylene can be taken as flexible and bio-polymers of interested lengths such as microtubules are semiflexible. There exist many famous models for describing the mechanic properties of a single polymer [1, 3–6], and three of them are listed here, two for flexible polymers and one for semiflexible polymers.

- **Gaussian chain**. By assuming a flexible polymer with a bead-spring structure (shown in Figure 1.1a) where the lengths of the springs can fluctuate obeying a Gaussian distribution and the orientations of the springs are independent of the others, one can get the probability of finding the polymer which consists of N monomers (or springs in the bead-spring description) with the end-to-end vector, $\boldsymbol{R}' - \boldsymbol{R}$, as shown in Figure 1.1 [3], as: $P(\boldsymbol{R}' - \boldsymbol{R}; N) = \left(\frac{3}{2\pi N b^2}\right)^{3/2} \exp\left[-\frac{3(\boldsymbol{R}'-\boldsymbol{R})^2}{2Nb^2}\right]$, where b is the monomer size. Then the free energy of the polymer as a function of the end-to-end vector, $\boldsymbol{R}' - \boldsymbol{R}$, is: $F_\mathrm{gc} = \frac{3k_\mathrm{B}T}{2Nb^2}(\boldsymbol{R}' - \boldsymbol{R})^2$, which describes the Gaussian chain as a Hookean spring with the elastic constant: $k = 3k_\mathrm{B}T/Nb^2$. Straightforwardly, one can obtain the force-extension relation as:

$$f = \frac{3k_\mathrm{B}T}{Nb^2}|\boldsymbol{R}' - \boldsymbol{R}|. \tag{1.1}$$

  As noted, the Gaussian chain can be stretched infinitely with $|\boldsymbol{R}' - \boldsymbol{R}| \to \infty$ if the tensile force is large enough, which is not correct for realistic polymers. Actually, this model can only describe the cases where the polymer undergoes small deformations rather than finite ones, i.e., $|\boldsymbol{R}' - \boldsymbol{R}| \ll l_\mathrm{c}$.

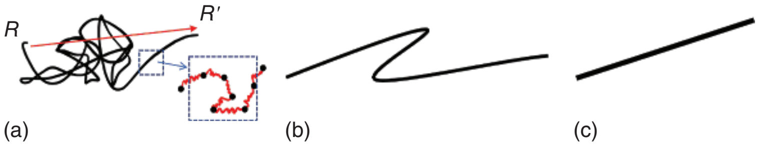

Figure 1.1 Illustration of a (a) flexible polymer ($l_\mathrm{c} \gg l_\mathrm{p}$) (the inset shows the bead-spring structure), (b) semiflexible polymer ($l_\mathrm{c} \simeq l_\mathrm{p}$), and (c) rigid polymer ($l_\mathrm{c} \ll l_\mathrm{p}$).

- **Langevin chain**. For a flexible polymer chain which is stretched finitely, $|\boldsymbol{R}' - \boldsymbol{R}| \sim l_c$, one can adopt the freely joint chain model, where the length of the springs in Figure 1.1a is a constant b (infinitely rigid and not deformable) and the orientation of each spring is independent of others. Then the force-extension relation can be obtained as [6]:

  $$|\boldsymbol{R}' - \boldsymbol{R}| = Nb\,\mathcal{L}(fb/k_\mathrm{B}T), \tag{1.2}$$

  where $\mathcal{L}(x) = \coth(x) - 1/x$ is the Langevin function. One can easily show that Equation (1.2) reduces to Equation (1.1) if $|\boldsymbol{R}' - \boldsymbol{R}| \ll l_c$.
- **Semiflexible chain**. For semiflexible polymer chains, one needs to consider the bending rigidity (the orientations of the springs are dependent on those of their neighbors if still taking the bead-spring picture for an intuitive understanding). A semiflexible polymer of contour length l_c can be coordinated as $\boldsymbol{r}(s)$ with $0 \le s \le l_c$ the arc length coordinate along the polymer, and the bending energy of the semiflexible polymer can be written as: $E_B = \frac{\kappa}{2}\int_0^{l_c} ds \left[\frac{d^2\boldsymbol{r}(s)}{ds^2}\right]^2$ where κ is the bending modulus, and $d^2\boldsymbol{r}(s)/ds^2$ is the local curvature at s. There are different models reviewed in Ref. [7, 8] for describing the elasticity of a single semiflexible polymer, such as *Marko-Siggia model* [9], *Ha-Thirumalai model* [10], *MacKintosh-Käs-Janmey model* [11], and *Blundell-Terentjev model* (shown below as an example) [12]. By taking the mean inextensibility assumption, one can obtain the free energy of a semiflexible polymer as a function of the end-to-end factor of the polymer $x = |\boldsymbol{R}' - \boldsymbol{R}|/l_c$, approximated as (details in Ref. [12]): $F_{sc}(x) = k_\mathrm{B}T\pi^2 c\left(1 - x^2\right) + \frac{k_\mathrm{B}T}{\pi c\left(1-x^2\right)}$, where $c = l_p/2l_c = \kappa/2k_\mathrm{B}Tl_c$ describes the bending rigidity of the polymer. From this, one can obtain the force-extension relation as:

  $$f = \frac{2k_\mathrm{B}T}{l_c}\left[-\pi^2 c + \frac{1}{\pi c\left(1 - x^2\right)^2}\right]x. \tag{1.3}$$

  Obviously, the force diverges at large $x \to 1$ when the polymer is stretched to its length limit.

With the mechanical models of a single polymer as exemplified above, one can try to construct theoretical models for macromolecular networks by taking account of the crosslinked structure of the network. The theories for a permanently crosslinked network have been developed for a relatively long time, and there are many successful models as reviewed in Ref. [13, 14]. The theoretical models of permanently crosslinked macromolecular networks can be roughly categorised into two types: statistical ones based on assumed network structures (Section 1.1.2) and phenomenological ones with fitting parameters well matching experimental observations (Section 1.1.3).

1.1.2 Statistical Models

With the mechanic models of a single polymer as shown above, one can try to construct the constitutive models of a macromolecular network with proper assumptions of the network structure. Here, we introduce four models with different network architectures, as shown in Figure 1.2.

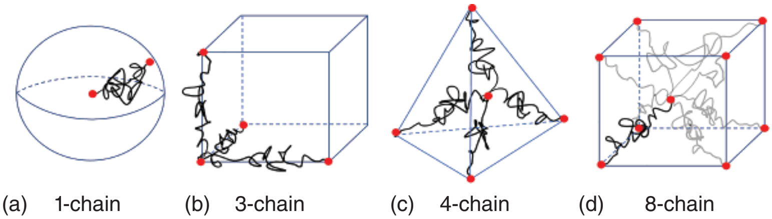

Figure 1.2 Four different architectures of macromolecular networks: (a) 1-chain model (full network model), (b) 3-chain model, (c) 4-chain model, (d) 8-chain model.

- **1-chain model (also called as full network model).** 1-chain model may be the most straightforward assumption of the network architecture, where the orientation of the polymer connecting two neighboring crosslinks (one located at the center of the sphere and the other at the sphere surface) is randomly distributed [15]. Then, the free energy density of the macromolecular network can be obtained by averaging the energy contributions of all polymers. Suppose the network is uniformly deformed, and the material point located at $\boldsymbol{r}$ is displaced to a new location $\boldsymbol{r}' = \mathbf{E} \cdot \boldsymbol{r}$ where $\mathbf{E}$ is the deformation gradient tensor. Note that $\mathbf{E}$ can be written as $\mathbf{E} = \mathbf{Q} \cdot \mathbf{S}$ with $\mathbf{Q}$ as an orthogonal tensor and $\mathbf{S}$ as a diagonal tensor; in other words, the deformation can be decomposed into a stretch denoted by $\mathbf{S}$ and a rotation denoted by $\mathbf{Q}$. The diagonal components ($\lambda_{1,2,3}$) of $\mathbf{S}$, satisfy the relation: $I_1 = \lambda_1^2 + \lambda_2^2 + \lambda_3^2 = E_{\alpha\beta}^2$ where I_1 is the first invariant which will be used later. Upon deformations, the sphere of radius ξ (denoting the mesh size of the network) will be deformed into an ellipsoid, where the lengths of the three semi-axes become $\lambda_1\xi$, $\lambda_2\xi$, and $\lambda_3\xi$, respectively. The energy density of the network can be calculated as:

$$F_{1\text{c}} = n_\text{c} \int \sin\theta d\theta\, d\varphi F_\text{chain}[\lambda(\theta,\varphi)\,\xi]/4\pi, \tag{1.4}$$

  where n_c is the density of the subchains (polymers connecting two neighboring crosslinks), $\lambda(\theta,\varphi) = \sqrt{\sin^2\theta(\cos^2\varphi\lambda_1^2 + \sin^2\varphi\lambda_2^2) + \cos^2\theta\lambda_3^2}$ is the deformation ratio at orientation (θ, φ), and F_chain is the energy density of a single polymer, which can be that of Gaussian chain model, Langevin chain model, semiflexible chain model, etc. Then, by averaging the contributions of all polymers, one can obtain the free energy density of the macromolecular network. However, it is usually not possible to obtain an analytic form of the free energy of the network consisting of the non-Gaussian polymers due to the complexity lying in the integration of the polar and azimuthal angles in the spherical coordinate system. The exception is the macromolecular networks of Gaussian polymers ($F_\text{chain} \propto \frac{3}{2}k_\text{B}T\lambda^2$), of which the free energy density can be explicitly obtained as:

$$F_{1\text{c}} = \frac{1}{2}G\left(\lambda_1^2 + \lambda_2^2 + \lambda_3^2 - 3\right), \tag{1.5}$$

  where G is the shear modulus of the material as a function of n_c; this energy form is also called as neo-Hookean model.

- **3-chain model.** In the 3-chain model [16], a non-deformed macromolecular network is composed of repeated cubic cells; in each cell, the cell edges of length l_0 denote polymer chains, and the cell vertices denote crosslinks. Upon deformations, the cubic becomes a cuboid, where the directions of the edges are along the principle directions of the deformation and the lengths of three orthogonal edges become $\lambda_1 l_0$, $\lambda_2 l_0$, $\lambda_3 l_0$, respectively. Then, by averaging the energy contributions of these three orthogonal chains, one can obtain an analytical form of the free energy density of the macromolecular networks as:

  $$F_{3c} = \frac{1}{3} n_c \sum_i F_{\text{chain}}(\lambda_i). \tag{1.6}$$

  Note that the three orthogonal chains can be deformed with different stretch ratios. The advantage of the 3-chain model (also of 8-chain model) is that: one can write down the analytic form of the free energy density of the macromolecular network as long as the explicit form of the free energy of a single chain exists.
- **4-chain model.** In the 4-chain model, the macromolecular network is composed of repeated regular tetrahedrons before deformation, which was first proposed by Flory and Rehner [17]. In each tetrahedron, there are five crosslinks (four at the vertices and one in the tetrahedron body whose position can fluctuate) and four chains (connecting the center crosslink and each vertex crosslink). Upon deformation, the four vertices are deformed to new positions affinely with the applied deformation. The free energy density of the network can be obtained by averaging the contributions of the four deformed chains. However, due to several factors such as the non-affine displacement of the center crosslink, fluctuation of the center crosslink relying on the strains, etc., one can not write down an analytical form of the free energy density of the macromolecular networks, which needs to be calculated numerically. We shall not introduce the calculations in detail, and interested readers can refer to Ref. [13, 18].
- **8-chain model.** Similarly as the 3-chain model, the macromolecular network is also treated as repeated cubes before deformation and the cubes becomes cuboid after deformation in the 8-chain model [19]. The difference between the 8-chain model and 3-chain model lies in the chain and crosslink arrangements in the cube: there are nine crosslinks in each cube for the 8-chain model (eight at the cube vertices and one at cube center) and eight polymer chains connecting the center crosslink and each vertex crosslink (no chain along the edge anymore). Note that all polymers are deformed identically in this model and their energy is a function of the stretch ratios along the three orthogonal directions. The free energy density of the macromolecular network in this model is simply:

  $$F_{8c} = n_c F_{\text{chain}}(\lambda_{1,2,3}), \tag{1.7}$$

  where F_{chain} is chosen according to the properties of a single polymer as in other models.

One can also adapt the network architectures to meet realistic demands in theoretical modeling, for example, one can show the microscopic physical picture in Mullins effect by introducing changes in the chain contour lengths with deformations [20]. Also, by introducing a nonuniform size distribution of the unit cell or proposing other more realistic network architectures, one can try to study the non-affine deformation in real macromolecular networks.

1.1.3 Phenomenological Models

There are many phenomenological models, which are constructed with fitting parameters to match the experimental observations and are usually portable to use. Here, we shall briefly introduce a very useful class: invariants-based continuum models. For describing the deformation of the material, we have introduced the deformation gradient tensor in the above section 1.1.2, based on which one can define the left Cauchy-Green deformation tensor as: $\mathbf{B} = \mathbf{E}\mathbf{E}^{\mathrm{T}}$. For isotropic materials, we can obtain the principle invariants [scalar valued function $I(\mathbf{B})$ with $I(\mathbf{B}) = I(\mathbf{Q} \cdot \mathbf{B} \cdot \mathbf{Q}^T)$ for all orthogonal tensor $\mathbf{Q}$] of the left Cauchy-Green deformation tensor:

$$I_1 = \mathrm{tr}\mathbf{B} = \lambda_1^2 + \lambda_2^2 + \lambda_3^2, \tag{1.8}$$

$$I_2 = \frac{1}{2}\left[(\mathrm{tr}\mathbf{B})^2 - \mathrm{tr}\mathbf{B}^2\right] = \lambda_1^2\lambda_2^2 + \lambda_2^2\lambda_3^2 + \lambda_3^2\lambda_1^2, \tag{1.9}$$

$$I_3 = \det\mathbf{B} = \lambda_1^2\lambda_2^2\lambda_3^2. \tag{1.10}$$

I_3 is equal to 1 for incompressible materials, which is usually the case for rubbers. Thus, the free energy of incompressible materials can be constructed in terms of I_1 and I_2. Rivlin proposed a general form of the free energy density based on the invariants, I_1 and I_2 [21]:

$$F_{\mathrm{R}} = \sum_{ij} C_{ij}(I_1 - 3)^i (I_2 - 3)^j, \tag{1.11}$$

where the coefficients C_{ij} are usually phenomenological parameters to be fitted with experimental data. It can act as a framework guiding how to construct continuum models based on invariants.

- **Neo-Hookean model.** From the above expression (Eq. (1.11)), one can immediately recognize that the case of $C_{10} \neq 0$ and other $C_{ij} = 0$ corresponds to the neo-Hookean model obtained above from statistical arguments,

  $$F_{\mathrm{nH}} = C_{10}(I_1 - 3), \tag{1.12}$$

  and the phenomenological parameter $C_{10} = n_{\mathrm{c}} k_{\mathrm{B}} T/2$ has its microscopic origin as described above.
- **Mooney–Rivlin model.** Another simple example is Mooney–Rivlin model, which reads as [22]:

  $$F_{\mathrm{MR}} = C_{10}(I_1 - 3) + C_{01}(I_2 - 3), \tag{1.13}$$

  and it is also widely used for mechanics of rubber materials at small deformations.

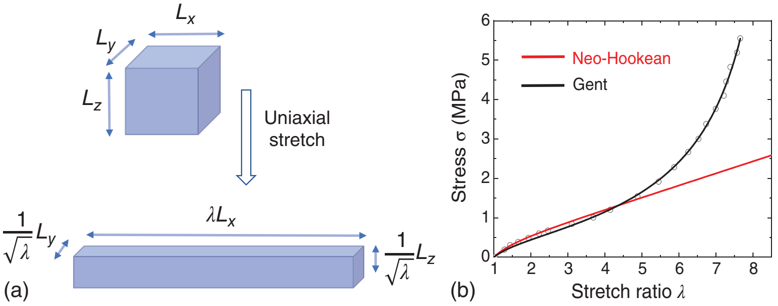

Figure 1.3 (a) Uniaxial stretch test, where the stretch ratio along the stretch direction is λ and the stretch ratios along the other two orthogonal directions are identical, which is equal to $1/\sqrt{\lambda}$ due to incompressibility of the material. (b) Stress–strain relation of the uniaxial stretch test, where the symbols denote the data extracted from the experiment. Source: Adapted from Treloar [13]. The red curve is fitted with the neo-Hookean model (fitting parameter $G \approx 0.30$ MPa), and the black curve is fitted with Gent model (fitting parameters $G \approx 0.25$ MPa and $J_\mathrm{m} \approx 85$).

- **Gent model.** When macromolecular networks undergo large deformations, there is a very good phenomenological model for describing the mechanics of them–Gent model [23], with the free energy density defined as:

  $$F_\mathrm{G} = -\frac{G}{2} J_\mathrm{m} \ln\left(1 - \frac{I_1 - 3}{J_\mathrm{m}}\right), \tag{1.14}$$

  where J_m characterizes the finite stretchability of the macromolecular networks, and one can show that the Gent model reduces to neo-Hookean model for small deformations, i.e., $I_1 - 3 \to 0$. Figure 1.3 shows the comparison of the experiment with the neo-Hookean/Gent model. By performing Taylor expansion of Eq. (1.14), one can notice that Gent model is still a specific form of Rivlin framework as shown in Eq. (1.11). Such models incorporating the finite stretchability of the materials can be applied to understand instabilities in rubber systems [24, 25].

There are other models based on tensor invariants, which we shall not show them here for saving space, and interested readers can refer to Ref. [14].

Apart from the above models based on invariants of the left Cauchy–Green tensor, there are many other types of phenomenological models, e.g., stretch-based models which include the widely used Ogden model [26, 27]. For practical needs, one can choose the most convenient one to use.

1.2 Permanent Biomacromolecular Networks

Macromolecular networks widely exist in biological systems, such as cytoskeleton and extracellular matrices, and these networks are simply called as biomacromolecular networks here. In these networks, the consisting polymers are usually semiflexible, such as microtubules, actin filaments and vimentin filaments, and the crosslinks can be motor proteins. In reality, constructing elastic models of biomacromolecular networks is similar to that of flexible macromolecular networks, as discussed in Section 1.1. We shall first show several useful elastic models of biomacromolecular networks in Section 1.2.1 and then focus on how to apply them to analyze the characteristic properties of these networks which make them special from flexible ones in Section 1.2.2.

1.2.1 Elastic Models

Here we shall introduce several elastic models of biomacromolecular networks which are widely used for understanding their mechanical properties, which are reviewed in Ref. [7, 8].

- **Storm et al. model.** Suppose that **E** is the deformation gradient tensor and $\rho \sim 1/\xi^2$ is the polymer length per unit volume (ξ denotes mesh size), a measure of network density. After deformation, the length density of the semiflexible polymers per unit volume which cross the plane perpendicular to j axis would change to $\rho E_{jk} n_k / \det \mathbf{E}$, where **n** is the orientation of the end-to-end vector of the polymer in an initially undeformed network, and $\det \mathbf{E}$ can measure the relative volume change of the deformed network. The tension acting on the polymer which connects two neighboring crosslinks is: $f(|\mathbf{E} \cdot \mathbf{n}| - 1)$, where $|\mathbf{E} \cdot \mathbf{n}| - 1$ is the axial strain of the filament, and $f(|\mathbf{E} \cdot \mathbf{n}| - 1)$ denoting the force-extension relationship of the polymer can be chosen from the models discussed in the above section. The stress tensor can then be obtained as a function of the strain tensor [3, 28]:

$$\sigma_{ij} = \frac{\rho}{\det \mathbf{E}} \left\langle f(|\mathbf{E} \cdot \mathbf{n}| - 1) \frac{\mathrm{E}_{il} n_l \mathrm{E}_{jk} n_k}{|\mathbf{E} \cdot \mathbf{n}|} \right\rangle . \tag{1.15}$$

- **8-chain model.** By assuming the 8-chain network architecture, similarly as that of flexible macromolecular networks, one can immediately know that all eight chains in the cube are stretched in the same way, with the length changing from $\sqrt{3}\xi/2$ (ξ denotes the edge length of the cube before deformation) to $\sqrt{I_1}\xi/2$. Palmer and Boyce provided the free energy density of the deformed macromolecular network as [29]:

$$F_{8\mathrm{c}}(I_1) = n_\mathrm{c} F_\mathrm{chain}(\sqrt{I_1/3}\xi). \tag{1.16}$$

  where n_c denotes the chain density and F_chain denotes the free energy of a single semiflexible polymer. Based on the free energy, one can obtain the constitutive relation describing the elasticity of the networks.

- **3-chain model.** In 2016, the free energy density of the biomacromolecular network is obtained based on the 3-chain architecture of the network [30]. The analytic form of the free energy density is:

$$F_{3\mathrm{c}}(\{\lambda_{i=1,2,3}\}) = \frac{n_\mathrm{c}}{3} \sum_{i=1,2,3} F_\mathrm{chain}(\lambda_i \xi) = \frac{n_\mathrm{c} k_\mathrm{B} T}{3} \times \left[\pi^2 c \left(3 - x^2 I_1\right) + \frac{3 - 2I_1 x^2 + I_2 x^4}{\pi c \left(1 - I_1 x^2 + I_2 x^4 - I_3 x^6\right)} \right], \tag{1.17}$$

where $c = l_p/2l_c$ and $x = \xi/l_c$ are defined in Eq. (1.3). From the free energy of the biomacromolecular network, one can obtain the constitutive relation as [31]:

$$\sigma_{ij} = 2\left[\left(\frac{\partial F_{3c}}{\partial I_1} + I_1\frac{\partial F_{3c}}{\partial I_2}\right)\mathrm{B}_{ij} - \left(I_1\frac{\partial F_{3c}}{\partial I_1} + 2I_2\frac{\partial F_{3c}}{\partial I_2}\right)\frac{\delta_{ij}}{3} - \frac{\partial F_{3c}}{\partial I_2}\mathrm{B}_{ik}\mathrm{B}_{kj}\right] - P\delta_{ij}, \tag{1.18}$$

where $\mathbf{B} = \mathbf{E}\mathbf{E}^{\mathrm{T}}$ is the left Cauchy-Green deformation tensor, and P is the Lagrangian multiplier in charge of the assumed incompressibility, the value of which can be determined by the boundary conditions.

In the next section, the 3-chain model is taken as an example to analyze the elastic properties of biomacromolecular networks.

1.2.2 Nonlinear Elasticity, Stability, and Normal Stress

When a biomacromolecular network undergoes deformations, e.g., a simple shear, the networks can exhibit very different mechanic responses compared with flexible macromolecular networks. Here we shall show how to analyze the characteristic properties of the biomacromolecular networks by taking the 3-chain model as an example for describing the free energy of the networks.

- **Nonlinear elasticity.** For a biomacromolecular network undergoing a simple shear deformation denoted by the deformation gradient tensor as:

$$\mathbf{E} = \begin{pmatrix} 1 & \gamma & 0 \\ 0 & 1 & 0 \\ 0 & 0 & 1 \end{pmatrix}, \tag{1.19}$$

where γ is the shear strain, the stress–strain relation in the 3-chain model for the network of given parameters (x, c) can be explicitly written as [30]:

$$\left[\sigma_{xy}\right]_{3c}(\gamma; x, c) = \frac{2}{3}nk_{\mathrm{B}}T\gamma x^2\left[\frac{\left(1-x^4\right)}{c\pi\left[1-\left(2+\gamma^2\right)x^2+x^4\right]^2} - c\pi^2\right], \tag{1.20}$$

from which one can know that the stress is a linear function of the shear strain for small strains ($\sigma_{xy} \propto \gamma$ at $\gamma \to 0$), and diverges at a finite strain $\gamma_c = 1/x - x$, as shown in Figure 1.4a. There are two definitions of the shear modulus: nominal shear modulus $G(\gamma) = \sigma_{xy}(\gamma)/\gamma$ and differential shear modulus $K(\gamma) = \partial\sigma_{xy}/\partial\gamma$, which are identical at $\gamma \to 0$. An interesting mechanic property of biomacromolecular networks is about the relationship between the differential shear modulus K and the shear stress σ_{xy}, which is found to show a universal scaling at large strains $K \propto \sigma_{xy}^{3/2}$ (shown in Figure 1.4b). When the strain is approaching the divergence point $\gamma \to \gamma_c = 1/x - x$, then the stress and the differential shear modulus can be approximated as:

$$\sigma_{xy}(\gamma) \simeq nk_{\mathrm{B}}T\frac{2\gamma x^2(1-x^4)}{3\pi c\left[1-(2+\gamma^2)x^2+x^4\right]^2}, \tag{1.21}$$

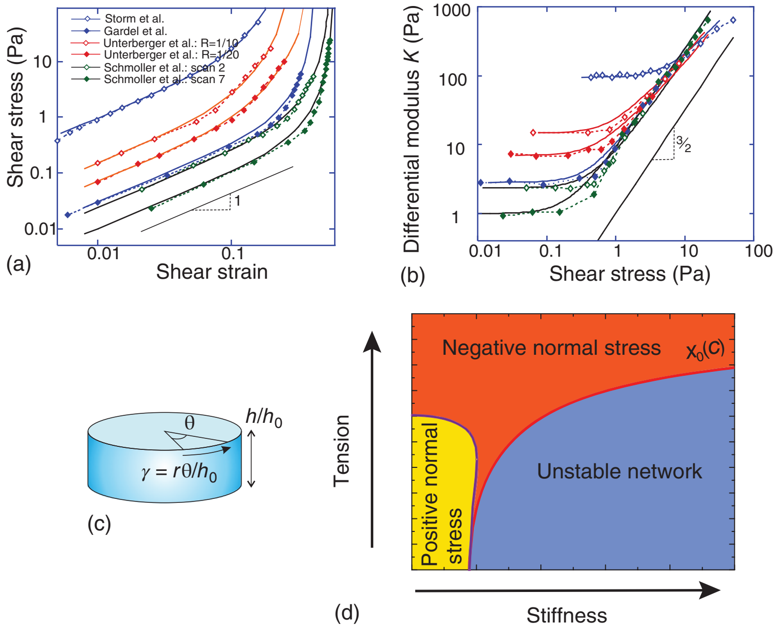

Figure 1.4 (a) Stress–strain relation of sheared biomacromolecular networks, with dots from different experiments. Source: Adapted from [28, 32–34]. And lines obtained by fitted Eq. (1.20). (b) Relationship between differential shear modulus and shear stress, which exhibit 3/2 scaling at large stresses [same data source as (a)]. (c) Twisting deformation of the biomacromolecular network and the phase diagram showing positive/negative normal stress regions in the plane of (biomacromolecule stiffness and pre-tension) and the unstable region. Source: The figure is adapted from Ref. [30].

$$K(\gamma) \simeq nk_BT\frac{2(1-x^4)\left[x^2-(2-3\gamma^2)x^4+x^6\right]}{3\pi c\left[1-(2+\gamma^2)x^2+x^4\right]^3}, \tag{1.22}$$

from which one can easily notice $K \propto \sigma_{xy}^{3/2}$. This 3/2 scaling actually originates from the mechanic properties of a single biopolymer (semiflexible), since there is the relation as: $d\sigma/d\gamma \sim df/dx \sim 1/(1-x^2)^3 \sim f^{3/2}$ at $x \to 1$ (f denotes force) from the elastic model of a single semiflexible polymer.

- **Network stability.** For a single biomacromolecule (semiflexible polymer), the relaxed state is given by x_0 satisfying zero-force condition $f(x_0) = 0$, and the value of x_0 depends on the rigidity of the polymer described by c. However, for a biomacromolecular network, the consisting polymers are not necessarily at the force-free states, in other words, the end-to-end factor x can be $>, <, = x_0$, meaning the network is in a prestretched, precompressed, and relaxed state, respectively. The criterion to judge whether a network of a given parameter set (x, c) is stable is given by the linear shear modulus (the constant modulus at small strains): $G_0 \geq 0$. In the 3-chain model, this condition can be expressed as [30]:

$$c \leq \frac{1}{\pi^{3/2}}\frac{\sqrt{1+x^2}}{(1-x^2)^{3/2}}. \tag{1.23}$$

Note that the right-hand side in Eq. (1.23) is always larger than $c^* = 1/\pi^{\frac{3}{2}}$, meaning that for sufficiently flexible chains with $c < c^*$, the network is always stable. On the other hand, for filament networks composed of the stiffer filaments with $c \geq c^*$, the network strands have to be crosslinked with x exceeding the pre-tension threshold given by Eq. (1.23), in order for the network to have a finite linear shear modulus. In other words, there are usually forces acting on the crosslinked filaments in the network in order to be mechanically stable with a non-zero shear modulus.

- **Normal stress.** Consider a cylindrical macromolecular network which is subjected to a twist deformation, as shown in Figure 1.4c. For typical rubbers, the height of the cylinder (length along the longitudinal direction) increases together with a decrease in its radius, and this phenomenon is called as "positive Poynting effect" corresponding to a positive normal stress [35, 36]. However, a biomacromolecular network usually behaves oppositely, i.e., its height decreases and radius increases, showing the "negative Poynting effect" which corresponds to a negative normal stress [37]. Suppose the height and the radius of the undeformed cylinder are h_0 and R_0, respectively, which change to $h = \lambda_h h_0$ and $R = \lambda_R R_0$ after being twisted with $\lambda_{h,R}$ as the stretch ratio along the longitudinal and the radial directions, respectively ($\lambda_h \lambda_R^2 = 1$ due to the incompressibility of the material). In the cylindrical coordinate system, the material point at (r, θ, z) changes its position to $(r/\sqrt{\lambda_h}, \theta + \Theta z/h_0, \lambda_h z)$ after rotating the top plate with angle Θ, and the deformation gradient tensor of the macromolecular network can be expressed as:

$$\mathbf{E} = \begin{pmatrix} 1/\sqrt{\lambda_h} & 0 & 0 \\ 0 & 1/\sqrt{\lambda_h} & \gamma(r)/\sqrt{\lambda_h} \\ 0 & 0 & \lambda_h \end{pmatrix}, \tag{1.24}$$

where $\gamma(r) = r\Theta/h_0$ is the shear strain depending on the radial position. Given the shear strain at the outermost surface, $\gamma_0 = \gamma(R_0)$, the total free energy of the deformed network can be expressed as a function of the stretching ratio λ_h along the z-axis after integration over the radius [30],

$$F_{\text{cylinder}}(\lambda_h; \gamma_0) = \int_0^{R_0} dr F_{3c}(\lambda_h, r; \gamma_0). \tag{1.25}$$

By minimizing the above free energy, we can obtain the optimal λ_h, which can tell us whether the material shows positive or negative Poynting effect. The phase diagram in the space of (c, x) is shown in Figure 1.4d, where the boundary line separating the positive/negative normal stress regions is given. It is clear from the phase diagram that a sheared flexible network with $c < c^* = 1/\pi^{\frac{3}{2}}$ usually shows a positive normal stress, while a semiflexible filament network exhibits a negative normal stress.

In this section, we have introduced useful theoretical models of the *permanent* macromolecular/biomacromolecular networks, which can be utilized for analyzing the characteristic elastic properties.

1.3 Transient Macromolecular/Biomacromolecular Networks

Transient macromolecular/biomacromolecular networks are important in both industrial applications and biological systems, as reviewed in Ref. [38, 39]. In transient networks, the crosslinks usually can break and re-form dynamically at high temperatures, so the network shape (and microscopic structure) can be altered; meanwhile, at low temperatures, the crosslinks are stable so that the network just act as a permanent one as described in the above section. Such dynamic crosslinks can be either physical which is formed by physical interactions (hydrogen bonds, guest–host interactions, hydrophobicity, protein–protein interactions, etc.), or chemical covalent bonds where polymer chains exchange by transesterification reaction, transamination of vinylogous urethanes, etc. In industry, such transient feature of crosslinks allows the networks to behave as thermoplastics at high temperatures which are remoldable and recyclable, and then as thermosets at low temperatures showing excellent mechanic properties. In bio-systems, the transient crosslinks such as motor proteins enable the biomacromolecular networks to change their structures accordingly for accommodating to different mechanical or chemical environments.

The theoretical studies of transient macromolecular networks have a long history, which can be roughly categorized into statistical and macroscopic ones, as recently reviewed in Ref. [40]. For statistical works based on the dynamic evolution of polymer chains (with dynamic breakage from and re-crosslinked to the crosslinks), one can analyze the viscoelasticity of the networks. Such studies can date back to the work by Green and Tobolsky [41], where they introduced the breakage and the re-formation of the crosslinks for understanding the relaxation of the polymer networks. Following this, a consistent framework for treating the crosslink dynamics subjected to external forces was constructed with the representative works by Tanaka and Edwards in 1990s and then further developed recently [42–49]. In such models, the crosslink dynamics depend on the loadings on the polymer chains, which can be explicitly expressed in terms of the deformations. Separately, the concepts of Rouse dynamics and reptation were used for studying the dynamics of a transient network by Leibler et al. [50], and also by Rubinstein and Semenov [51]. For macroscopic models, Drozdov et al. developed continuum models for various systems involving transient networks, where the crosslink dynamics can be expressed in terms of the energy density with fitting parameters [52–54]. Similar ideas were further developed and successfully applied to deal with dual networks by Long and Hui et al. [55–57]. Apart from these, there are also theoretical works on modeling how the viscoelasticity of the transient macromolecular networks depend on the nonaffinity of the network [46, 53], network defects [58], crosslinker mobility [59], multifunctional crosslink dynamics [60], etc.

Following Tanaka–Edwards model, we shall introduce a microscopic-macroscopic hybrid model in this section, where the microscopic crosslink dynamics depending on the mechanic forces acting on the polymer chains is incorporated into a macroscopic continuum theory (Figure 1.5).

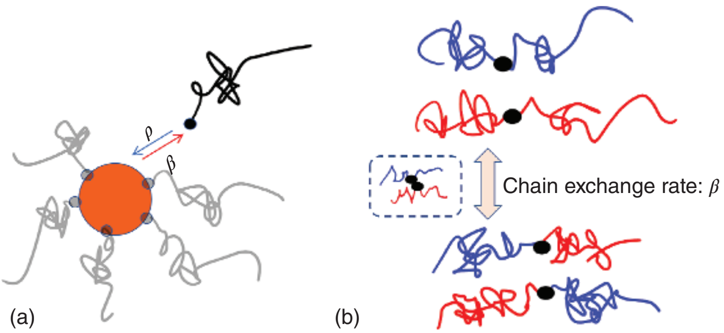

Figure 1.5 Schematics of (a) a physical crosslink where chains can dynamically break from and re-attach to, and (b) a chemical crosslink where chains can dynamically exchange.

1.3.1 Theoretical Framework

We here introduce the modeling of physically crosslinked transient macromolecular networks, and it can be easily generalized to chemical ones, for which we shall talk about vitrimers [a new type of associative covalent adaptive networks (CAN)] as an example. Suppose the energy barrier for a *flexible* polymer to break from a crosslink is W_b, and then the rate for a relaxed chain to break from its bonded crosslink is: $\beta_0 = \omega_0 \exp(-W_b/k_\mathrm{B}T)$, which increases to $\beta = \omega_0 \exp[(-W_b + fb)/k_\mathrm{B}T]$ when the chain experiences a tensile force f lowering the energy barrier [45]. Note that the force is tensile for *flexible* polymer, i.e., $f > 0$; for *semiflexible* polymers, one may need to use the absolute value of f, i.e., $|f|$, since it can be stretched or compressed. Correspondingly, one can define the re-crosslinking rate for a dangling polymer to be crosslinked: $\rho_0 = \omega_0 \exp(-W_c/k_\mathrm{B}T)$ with W_c as the re-crosslinking barrier; note that in cases of physical crosslinks, the practical re-crosslinking rate is usually much smaller than ρ_0 as the dangling polymer needs to diffuse to "find" the crosslink and the effective re-crosslinking rate is $\rho = 1/(\tau + 1/\rho_0)$ where τ is the diffusion time. The newly crosslinked chains are assumed to be relaxed, i.e., their reference state needs to be defined according to when they are crosslinked.

Suppose there are N_0 chains in the polymer network, where at time t the number of the crosslinked chains is $N_\mathrm{c}(t)$ and the number of the dangling chains is $N_\mathrm{b}(t) = N_0 - N_\mathrm{c}(t)$. After an infinitesimal time interval Δt, the number of the initially crosslinked chains decreased to $N_\mathrm{c}(0)\exp(-\beta\Delta t)$, and meanwhile, there are chains which are newly crosslinked to the network, of which the number is $N_\mathrm{b}(0)\rho\Delta t$; the total number of crosslinked chains is: $N_\mathrm{c}(0)\exp[-\beta(\Delta t;0)\Delta t] + N_\mathrm{b}(0)\rho\Delta t$. Note that the breakage rate $\beta(t;t')$ depends both on the initial time t' when the chain is crosslinked and the current time t, since the forces acting on the chains depend on the deformation referenced to when the chains get crosslinked. After another time interval, the number of the chains remaining crosslinked at $t = \Delta t$ decreases to $N_\mathrm{c}(0)\exp[-\beta(\Delta t;0)\Delta t]\exp[-\beta(2\Delta t;0)\Delta t] + N_\mathrm{b}(0)\rho\Delta t\exp[-\beta(2\Delta t;\Delta t)\Delta t]$, and meanwhile, there are chains newly crosslinked to the network, of which the number is $N_\mathrm{b}(\Delta t)\rho\Delta t$; the total number of crosslinked chains becomes: $N_\mathrm{c}(0)\exp[-\beta(\Delta t;0)\Delta t]\exp[-\beta(2\Delta t;0)\Delta t] + N_\mathrm{b}(0)\rho\Delta t\exp[-\beta(2\Delta t;\Delta t)\Delta t] + N_\mathrm{b}(\Delta t)$

$\rho\Delta t$. By repeating the above calculations, the total number of the crosslinked chains after N time intervals becomes: $\prod_{l=1}^{N} N_\mathrm{c}(0)\exp[-\beta(l\Delta t; 0)\Delta t] + \sum_{m=1}^{N} N_\mathrm{b}((m-1)\Delta t)\Delta t \prod_{l=m+1}^{N} \exp[-\beta(l\Delta t; m\Delta t)\Delta t]$, which can be written in a continuous form:

$$N_\mathrm{c}(t) = N_\mathrm{c}(0)\, e^{-\int_0^t dt'\, \beta(t';0)} + \int_0^t dt'\, N_\mathrm{b}(t)\, \rho\, e^{-\int_{t'}^t dt''\, \beta(t'';t')}. \tag{1.26}$$

Consider the fact that the relaxed chains are almost isotropically distributed, then the free energy of the network can be regarded as the summation of that of all polymers, as what Tanaka and Edwards did in their papers [44, 45]. As mentioned in the previous sections on permanent macromolecular networks, it is usually difficult (or impossible) to obtain an analytical expression of the free energy of a macromolecular network by statistically averaging the contributions of the polymers which distributed uniformly in all possible directions, and this is also the case for transient macromolecular networks. So, one needs to make simplifications in order to obtain a compact form of the free energy of a transient macromolecular network; the network can be treated as an assembly of subnetworks which form at different time according to when the chains get crosslinked. Then the free energy density of the transient polymer network can be expressed as [61]:

$$F_\mathrm{tr}(t) = e^{-\int_0^t dt'\, \beta(t';0)} F_\mathrm{per}(t;0) + \int_0^t dt'\, \frac{N_\mathrm{b}(t)}{N_\mathrm{c}(0)} \rho\, e^{-\int_{t'}^t dt''\, \beta(t'';t')} F_\mathrm{per}\left(t;t'\right), \tag{1.27}$$

where $F_\mathrm{per}(t;t')$ denotes the free energy density contributed by the subnetwork which forms at time t' (reference time), and its form can be taken from those of permanent macromolecular networks depending on the network properties.

1.3.2 Applications

In the following part, we shall show how to utilize the above theoretical framework to study the viscoelasticity of a transient macromolecular network by taking the uniaxial stretch test as an example, where the global deformation gradient tensor referenced at time $t = 0$ can be expressed as:

$$\mathbf{E}(t;0) = \begin{pmatrix} \lambda(t;0) & 0 & 0 \\ 0 & 1/\sqrt{\lambda(t;0)} & 0 \\ 0 & 0 & 1/\sqrt{\lambda(t;0)} \end{pmatrix}, \tag{1.28}$$

where λ denotes the stretch ratio along x direction and incompressibility of the network is assumed.

- **Small deformations.** When the transient macromolecular network consisting of flexible polymers undergoes a small deformation, i.e., $\lambda \to 1$, the consisting polymers can be treated as Gaussian chains and the form of the free energy density of the permanent network can be taken as that of neo-Hookean model, $F_\mathrm{per}(t;t') = \frac{1}{2}G[\lambda(t;t')^2 + 2/\lambda(t;t') - 3] = \frac{1}{2}G[\lambda(t)^2/\lambda(t')^2 + 2\lambda(t')/\lambda(t) - 3]$, where the relation for the deformation gradient tensor $\mathbf{E}(t;t') = \mathbf{E}(t;0)\mathbf{E}^{-1}(t';0)$ is utilized. Meanwhile, the breakage rate depends on the force acting on the polymer, where the force is a function of the end-to-end distance of the polymer (the distance r depends on when the polymer is crosslinked to the network and the deformation of the network), $f = \frac{3k_BT}{Nb^2}r$. Here, we can use the averaged end-to-end distance of the polymers distributed uniformly in all possible directions to obtain an approximate value of the breakage rate $\beta(t;t') = \omega_0 \exp[(-W_b + 3k_BT\langle r\rangle/Nb)/k_BT] = \beta_0 \exp[3\langle r\rangle/Nb]$, and it increases with the stretch ratio λ as shown in Ref. [61, 62]. The stress–strain relation in this case can be explicitly expressed as [61]:

$$\sigma_{xx}(t) = Ge^{-\int_0^t dt'\,\beta(t';0)}\left[\lambda(t) - \frac{1}{\lambda(t)^2}\right] + G\int_0^t dt'\,\frac{N_b(t)}{N_0}\,\rho\,e^{-\int_{t'}^t dt''\,\beta(t'';t')} \times \left[\frac{\lambda(t)}{\lambda(t')^2} - \frac{\lambda(t')}{\lambda(t)^2}\right], \tag{1.29}$$

where the first term on the right-hand-side shows contributions of the polymers which are crosslinked at time $t = 0$ and remain crosslinked until time t, and the second term denotes the contributions of the polymers which are crosslinked at different time t' and remain crosslinked until time t during the deformation. Other stress components are *zero*. Here, we consider two cases. *Case (1)*: the network is instantaneously stretched and then kept with a constant stretch ratio λ_0. Then, the stress relaxes exponentially with time and the relaxation rate is equal to breakage rate; this is obvious from Eq. (1.29), where the first term on the right-hand-side shows the exponential decay of the stress, and the second term has no contribution to the stress because of $\lambda(t) = \lambda(t') = \lambda_0$. Usually in realistic transient macromolecular networks, the stress relaxation does not follow a simple exponential function of time, but a stretched exponential function, $e^{-(\beta t)^\alpha}$ with the stretching factor $\alpha < 1$ depending on system properties, for example, a wide distribution of the energy barriers for crosslink breakage [61]. *Case (2)*: another common rheology test is strain ramp deformation, where the network is stretched with a constant strain rate, $\lambda(t) = 1 + \dot{\gamma}t$. The relationship between the stress and the strain/time can be obtained from Eq. (1.29), which is plotted in Figure 1.6 for different strain rates. For small strain rates, the stress first increases with the strain and then decreases, and the turnover is named as yielding point located at a small

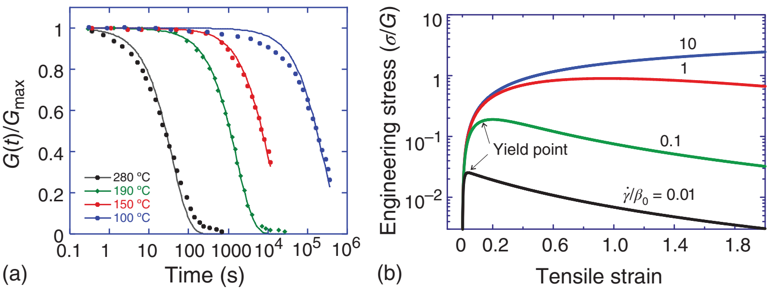

Figure 1.6 (a) Stress relaxation. Dots are from the experiment [63] and lines are obtained by fitting the exponential decay equation. (b) Stress–strain relation in the ramp deformation tests with different strain rates. Source: Ref. [61] American Chemical Society/CC BY 4.0.

strain $\gamma_y \simeq \dot{\gamma}/\beta$ (yielding time $t_y \simeq 1/\beta$). When the strain rate is large, then the stress–strain relation is similar to that of a permanent macromolecular network, since most of the initially crosslinked chains have not broken from the crosslinks at small strains.

- **Large deformations.** When the transient macromolecular networks consisting of flexible polymers undergo a large deformation, Gent model is usually taken for describing the energy density of the permanent macromolecular networks, which is $F_{\mathrm{per}}(t;t') = -\frac{1}{2}GJ_{\mathrm{m}}\ln[1-\frac{J(t;t')}{J_m}]$ with $J(t;t') = \lambda^2(t;t') + 2/\lambda(t;t') - 3$, and the stress–strain relationship is [64]:

$$\sigma_{xx} = \frac{GJ_{\mathrm{m}}}{J_{\mathrm{m}} - J(t;0)}\left[\lambda(t) - \frac{1}{\lambda(t)^2}\right] e^{-\int_0^t \beta(t';0)dt'} + \int_0^t \rho \frac{GJ_{\mathrm{m}}}{J_{\mathrm{m}} - J(t;t')}\left[\frac{\lambda(t)}{\lambda(t')^2} - \frac{\lambda(t')}{\lambda(t)^2}\right] \frac{N_{\mathrm{b}}(t')}{N_0} e^{-\int_{t'}^t \beta(t'',t')dt''} dt'. \tag{1.30}$$

Note that there is a divergence point, $J(t;0) \to J_{\mathrm{m}}$, where the stress diverges upon deformation. In the *stress relaxation* test, the stress of the network decreases exponentially with time in the same way as in the case of small deformations. In the *strain ramp deformation* test, the stress–strain relationship of the transient macromolecular networks becomes more interesting as shown in Figure 1.7a. When

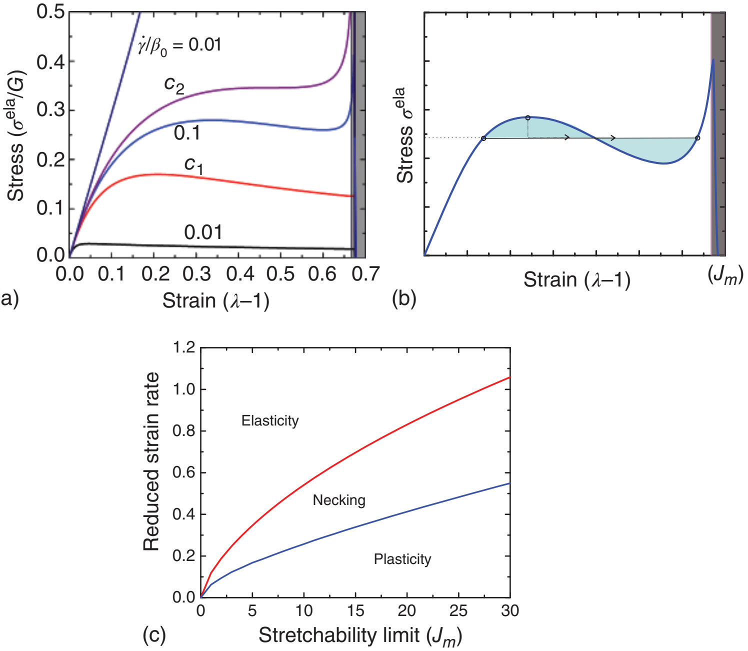

Figure 1.7 (a) Stress–strain relation in the ramp deformation tests with different strain rates. (b) A schematic of "S-shaped" stress–strain relation. (c) Phase diagram showing different viscoelastic responses of the transient macromolecular networks (elastic, plastic, or necking) in the plane of (stretchability limit, strain rate). Source: The figure is adapted from Ref. [64].

the strain rate is large, the stress increases with the strain until the divergence point, resembling that of a permanent macromolecular network. When the strain rate is small, the stress first increases and then decreases, similarly as that in the small deformation case. When the strain rate is moderate, the stress first increases, then decreases (turnover at the yielding point), and then increases again until the divergence point; such "S-shaped" stress–strain relation indicates the possibility to have two co-existing phases (one with large λ and the other with small λ, as necking instability) during the deformation if the energy barrier to create the interface between the two phases is not high (Figure 1.7b). The different responses of the transient macromolecular networks in the ramp deformation test are shown in the phase diagram (Figure 1.7c).

- **A special example: vitrimers.** Since Leibler et al. discovered a new type of associative CAN, which is named as vitrimers [63], such materials quickly attracted increasing attentions (reviewed in [65]); these materials exhibit characteristic properties including (i) the number of the crosslinks remains constant as other associative CAN and (ii) thermal viscosity changes with temperature in the form of Arrhenius law as inorganic silica materials. The covalently crosslinked polymers in vitrimers can dynamically exchange when adding catalysts or increasing temperature, and such bond exchange reactions can be implemented by transesterification reaction [63, 66], transamination of vinylogous urethanes [67], etc. Differently from the crosslink breakage and re-formation dynamics in physical transient networks, the exchangeable chains in vitrimers first associate and then dissociate, and one can treat that the crosslink breakage and re-formation occur simultaneously. The number of crosslinked chains can then be expressed as [68]:

$$N_c(t) = N_c(0)\, e^{-\beta t} + N_c(0) \int_0^t dt'\, \beta\, e^{-\beta(t-t')} \equiv N_c(0), \tag{1.31}$$

where the chain exchange rate β is taken as a constant for simplicity. As an obvious extension, the free energy of a dual network (two subnetworks, a transient one of fraction v and a permanent one of fraction $1 - v$) can be expressed as,

$$F_{\text{tr}}(t) = \left[v e^{-\beta t} + (1 - v) \right] F_{\text{per}}(t; 0) + v \int_0^t dt' \beta e^{-\beta(t-t')} F_{\text{per}}(t; t'), \tag{1.32}$$

where the reference state of the transient part changes with time. A detailed study about the rheological properties of the vitrimers in tests such as stress relaxation, strain ramp and creep, can be found in Ref. [68, 69].

- **Transient biomacromolecular networks.** In a biomacromolecular network, e.g., these existing in the form of cytoskeleton, the crosslinks such as bio-motors can dynamically attach to and detach from the biomacromolecules in the network, which endows the network with dynamic properties; in other words, the transient biomacromolecular network is a special example of macromolecular networks. Then by substituting the free energy density of the permanent biomacromolecular networks (examples given in Section 1.2.1) into Eq. (1.27), one can study how a transient biomacromolecular network responds to external mechanic stimuli [70]. Suppose that a transient biomacromolecular network is instantly stretched with the stretch ratio λ_0 and then kept stretched for a time interval τ, after which the tensile force is released and the network relaxes to a new state characterized by a new stretch ratio λ_r, which can be calculated by solving $\sigma_{\text{ela}}(\tau) = \sigma_0 e^{-\beta\tau} = \sigma\left(\lambda_0/\lambda_r(\tau)\right)$ [β is the breakage rate of the crosslinks as a function of λ_0] (Figure 1.8a). Then one can show that the recovery ratio (defined as $S(\tau) = \frac{\lambda_0-\lambda_r(\tau)}{\lambda_0-1}$) decreases with increasing τ due to the fact that the stress relaxes during this time period (shown in Figure 1.8b). In the strain ramp deformation, one finds that the "S-shaped" stress–strain relation of the material stretched with a moderate strain rate resembles that of flexible macromolecular networks undergoing large deformations, as shown in Figure 1.8c. Here, re-crosslinking is neglected, as it was shown in Ref. [61, 64] that re-crosslinking process usually alters the viscoelastic response of the materials in the ramp deformation test in a quantitative rather than qualitative way. Also, one can study how polydispersity in the mesh size of the network influences the viscoelasticity of the transient macromolecular networks, e.g., in the strain ramp deformation process, the network is softer at small strains and stiffer at large strains if the distribution of the mesh size is narrower as shown in Figure 1.8d, where one can assume the length of the polymer connecting two crosslinks l_c obeys a normal distribution $p(l_c) = (1/\sqrt{2\pi}\Delta)\exp[-(l_c - l_c^0)/2\Delta^2]$, with the expectation value l_c^0 and standard variance Δ as shown in (l_c has a correspondence with the mesh size $\xi(l_c)$ if the network resides in a stress-free state).

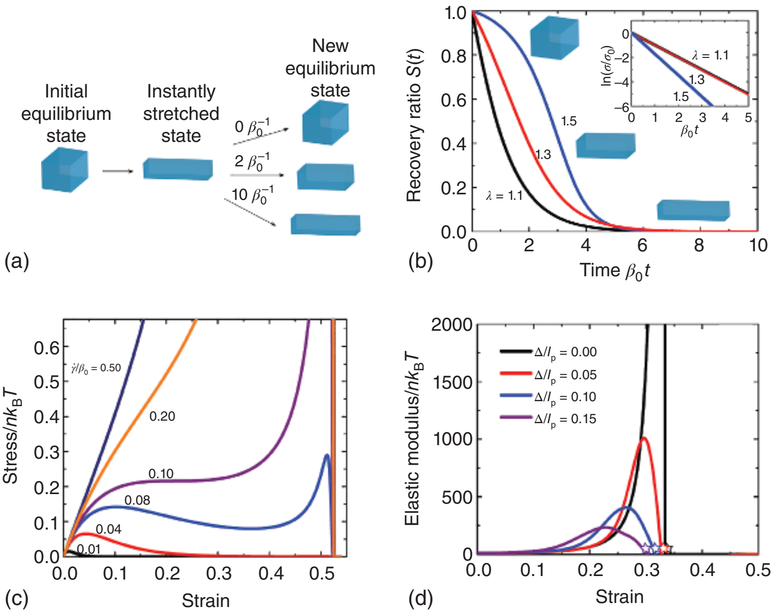

Figure 1.8 (a) Schematic showing the process of shape recovery and (b) the recovery ratio as a function of keeping time, where β_0 is the breakage rate of the crosslinks under the force-free condition (inset denotes the stress relaxation). (c) Stress–strain relationship in the ramp deformation test. (d) The evolution of modulus with applied strain in the ramp deformation test for networks of different distributions of mesh sizes. Source: Ref. [70]/ American Chemical Society.

In this section, we show how to model a transient macromolecular network including biological ones by incorporating the crosslink dynamics into a continuum theory, which can be applied to investigate the viscoelasticity of such interesting materials.

1.4 Outlooks

In this chapter, we have introduced several basic theories on macromolecular and biomacromolecular networks, which can be utilized to analyze the (visco)elasticity of different macromolecular network-based materials. These standard models can also be generalized to study other macromolecular systems, e.g., micro/nanocomposites [71, 72], ferrogels [73–75], electro-gels [76, 77], active gels [78], phase separation in polymer networks [79, 80], particle motion in a transient polymer network [81], exchangeable liquid crystal elastomers [82], etc. Interesting readers can refer to the literatures on these specific topics.

References

1 Flory, P.J. and Volkenstein, M. (1969). *Statistical Mechanics of Chain Molecules*. Wiley Online Library.

2 IUPAC (1997). *Compendium of Chemical Terminology*, 2e. Oxford: Blackwell Scientific Publications.

3 Doi, M. and Edwards, S.F. (1988). *The Theory of Polymer Dynamics*, vol. 73. Oxford University Press.

4 Rubinstein, M. and Colby, R.H. (2003). *Polymer Physics*. Oxford University Press.

5 Kawakatsu, T. (2004). *Statistical Physics of Polymers: An Introduction*. Springer Science & Business Media.

6 Doi, M. (2013). *Soft Matter Physics*. Oxford University Press.

7 Broedersz, C.P. and MacKintosh, F.C. (2014). Modeling semiflexible polymer networks. *Reviews of Modern Physics* 86: 995.

8 Meng, F. and Terentjev, E.M. (2017). Theory of semiflexible filaments and networks. *Polymers* 9: 52.

9 Marko, J.F. and Siggia, E.D. (1995). Stretching DNA. *Macromolecules* 28: 8759–8770.

10 Ha, B.-Y. and Thirumalai, D. (1997). Semiflexible chains under tension. *The Journal of Chemical Physics* 106: 4243–4247.

11 MacKintosh, F.C., Käs, J., and Janmey, P.A. (1995). Elasticity of semiflexible biopolymer networks. *Physical Review Letters* 75: 4425.

12 Blundell, J.R. and Terentjev, E.M. (2009). Stretching semiflexible filaments and their networks. *Macromolecules* 42: 5388–5394.

13 Treloar, LRG (1975). *The Physics of Rubber Elasticity*. Clarendon Press, Oxford.

14 Boyce, M.C. and Arruda, E.M. (2000). Constitutive models of rubber elasticity: a review. *Rubber Chemistry and Technology* 73: 504–523.

15 Wu, P.D. and Van Der Giessen, E. (1993). On improved network models for rubber elasticity and their applications to orientation hardening in glassy polymers. *Journal of the Mechanics and Physics of Solids* 41: 427–456.

16 Wang, M.C. and Guth, E. (1952). Statistical theory of networks of non-Gaussian flexible chains. *The Journal of Chemical Physics* 20: 1144–1157.

17 Flory, P.J. and Rehner, J. Jr. (1943). Statistical mechanics of cross-linked polymer networks I. Rubberlike elasticity. *The Journal of Chemical Physics* 11: 512–520.

18 Treloar, L.R.G. (1954). The photoelastic properties of short-chain molecular networks. *Transactions of the Faraday Society* 50: 881–896.

19 Arruda, E.M. and Boyce, M.C. (1993). A three-dimensional constitutive model for the large stretch behavior of rubber elastic materials. *Journal of the Mechanics and Physics of Solids* 41: 389–412.

20 Qian, D. and Meng, F. (2021). Modelling Mullins effect induced by chain delamination and reattachment. *Polymer* 222: 123608.

21 Rivlin, R.S. (1948). Large elastic deformations of isotropic materials IV. Further developments of the general theory. *Philosophical Transactions of the Royal Society of London. Series A* 241: 379–397.

22 Mooney, M. (1948). The thermodynamics of a strained elastomer. I. General analysis. *Journal of Applied Physics* 19: 434–444.

23 Gent, A.N. (1996). A new constitutive relation for rubber. *Rubber Chemistry and Technology* 69: 59–61.

24 Meng, F., Chen, J.Z.Y., Doi, M., and Ouyang, Z. (2014). Phase diagrams and interface in inflating balloon. *AIChE Journal* 60: 1393–1399.

25 Meng, F., Chen, J.Z.Y., Doi, M., and Ouyang, Z. (2015). The phase diagram and radial collapse of an inflated soft tube under twist. *Soft Matter* 11: 7046–7052.

26 Ogden, R.W. (1972). Large deformation isotropic elasticity–on the correlation of theory and experiment for incompressible rubberlike solids. *Proceedings of the Royal Society of London. Series A* 326: 565–584.

27 Ogden, R.W. (1997). *Non-Linear Elastic Deformations*. Courier Corporation.

28 Storm, C., Pastore, J.J., MacKintosh, F.C. et al. (2005). Nonlinear elasticity in biological gels. *Nature* 435: 191–194.

29 Palmer, J.S. and Boyce, M.C. (2008). Constitutive modeling of the stress–strain behavior of f-actin filament networks. *Acta Biomaterialia* 4: 597–612.

30 Meng, F. and Terentjev, E.M. (2016). Nonlinear elasticity of semiflexible filament networks. *Soft Matter* 12: 6749–6756.

31 Bower, A.F. (2009). *Applied Mechanics of Solids*. CRC Press.

32 Gardel, M.L., Shin, J.H., MacKintosh, F.C. et al. (2004). Elastic behavior of cross-linked and bundled actin networks. *Science* 304: 1301–1305.

33 Unterberger, M.J., Schmoller, K.M., Bausch, A.R., and Holzapfel, G.A. (2013). A new approach to model cross-linked actin networks: multi-scale continuum formulation and computational analysis. *Journal of the Mechanical Behavior of Biomedical Materials* 22: 95–114.

34 Schmoller, K.M., Fernandez, P., Arevalo, R.C. et al. (2010). Cyclic hardening in bundled actin networks. *Nature Communications* 1: 1–8.

35 Poynting, J.H. (1909). On pressure perpendicular to the shear planes in finite pure shears, and on the lengthening of loaded wires when twisted. *Proceedings of the Royal Society of London. Series A* 82: 546–559.

36 Mihai, L.A. and Goriely, A. (2011). Positive or negative poynting effect? The role of adscititious inequalities in hyperelastic materials. 467: Proceedings of the Royal Society A: Mathematical, Physical and Engineering Sciences, 3633–3646.

37 Janmey, P.A., McCormick, M.E., Rammensee, S. et al. (2007). Negative normal stress in semiflexible biopolymer gels. *Nature Materials* 6: 48–51.

38 Yang, Y. and Urban, M.W. (2013). Self-healing polymeric materials. *Chemical Society Reviews* 42: 7446.

39 Wei, Z., Yang, J.H., Zhou, J. et al. (2014). Self-healing gels based on constitutional dynamic chemistry and their potential applications. *Chemical Society Reviews* 43: 8114–8131.

40 Guo, Q. and Long, R. (2020). Mechanics of polymer networks with dynamic bonds. In: *Self-Healing and Self-Recovering Hydrogels*, Advances in Polymer Science, vol. 285 (ed. C. Creton and O. Okay), 127–164. Cham: Springer.

41 Green, M.S. and Tobolsky, A.V. (1946). A new approach to the theory of relaxing polymeric media. *The Journal of Chemical Physics* 14 (2): 80–92.

42 Fricker, H.S. (1973). On the theory of stress relaxation by cross-link reorganization. *Proceedings of the Royal Society of London. A. Mathematical and Physical Sciences* 335 (1602): 289–300.

43 Baxandall, L.G. and Edwards, S.F. (1988). Deformation-dependent properties of polymer networks constructed by addition of crosslinks under strain. *Macromolecules* 21 (6): 1763–1772.

44 Tanaka, F. and Edwards, S.F. (1992). Viscoelastic properties of physically crosslinked networks. 1. Transient network theory. *Macromolecules* 25 (5): 1516–1523.

45 Tanaka, F. and Edwards, S.F. (1992). Viscoelastic properties of physically crosslinked networks: Part 1. Non-linear stationary viscoelasticity. *Journal of Non-Newtonian Fluid Mechanics* 43 (2–3): 247–271.

46 Koga, T., Tanaka, F., Kaneda, I., and Winnik, F.M. (2009). Stress buildup under start-up shear flows in self-assembled transient networks of telechelic associating polymers. *Langmuir* 25: 8626–8638.

47 Vernerey, F.J., Long, R., and Brighenti, R. (2017). A statistically-based continuum theory for polymers with transient networks. *Journal of the Mechanics and Physics of Solids* 107: 1–20.

48 Brighenti, R. and Vernerey, F.J. (2017). A simple statistical approach to model the time-dependent response of polymers with reversible cross-links. *Composites Part B: Engineering* 115: 257–265.

49 Lamont, S.C., Mulderrig, J., Bouklas, N., and Vernerey, F.J. (2021). Rate-dependent damage mechanics of polymer networks with reversible bonds. *Macromolecules* 54 (23): 10801–10813.

50 Leibler, L., Rubinstein, M., and Colby, R.H. (1991). Dynamics of reversible networks. *Macromolecules* 24 (16): 4701–4707.

51 Rubinstein, M. and Semenov, A.N. (2001). Dynamics of entangled solutions of associating polymers. *Macromolecules* 34 (4): 1058–1068.

52 Drozdov, A.D. (1999). A constitutive model in finite thermoviscoelasticity based on the concept of transient networks. *Acta Mechanica* 133: 13–37.

53 Drozdov, A.D. and Christiansen, J.deC. (2006). Constitutive equations for the nonlinear viscoelastic and viscoplastic behavior of thermoplastic elastomers. *International Journal of Engineering Science* 44: 205–226.

54 Drozdov, A.D. and Christiansen, J.C. (2022). Tuning the viscoelastic response of hydrogel scaffolds with covalent and dynamic bonds. *Journal of the Mechanical Behavior of Biomedical Materials* 130: 105179.

55 Hui, C.-Y. and Long, R. (2012). A constitutive model for the large deformation of a self-healing gel. *Soft Matter* 8 (31): 8209–8216.

56 Long, R., Mayumi, K., Creton, C. et al. (2014). Time dependent behavior of a dual cross-link self-healing gel: theory and experiments. *Macromolecules* 47 (20): 7243–7250.

57 Guo, J., Liu, M., Zehnder, A.T. et al. (2018). Fracture mechanics of a self-healing hydrogel with covalent and physical crosslinks: a numerical study. *Journal of the Mechanics and Physics of Solids* 120: 79–95.

58 Ciarella, S., Sciortino, F., and Ellenbroek, W.G. (2018). Dynamics of vitrimers: defects as a highway to stress relaxation. *Physical Review Letters* 121: 058003.

59 Mulla, Y. and Koenderink, G.H. (2018). Crosslinker mobility weakens transient polymer networks. *Physical Review E* 98: 062503.

60 Ozaki, H. and Koga, T. (2020). Theory of transient networks with a well-defined junction structure. *The Journal of Chemical Physics* 152 (18): 184902.

61 Meng, F., Pritchard, R.H., and Terentjev, E.M. (2016). Stress relaxation, dynamics, and plasticity of transient polymer networks. *Macromolecules* 49: 2843–2852.

62 Serero, Y., Jacobsen, V., Berret, J.-F., and May, R. (2000). Evidence of nonlinear chain stretching in the rheology of transient networks. *Macromolecules* 33 (5): 1841–1847.

63 Montarnal, D., Capelot, M., Tournilhac, F., and Leibler, L. (2011). Silica-like malleable materials from permanent organic networks. *Science* 334: 965–968.

64 Meng, F. and Terentjev, E.M. (2016). Transient network at large deformations: elastic–plastic transition and necking instability. *Polymers* 8 (4): 108.

65 Denissen, W., Winne, J.M., and Du Prez, F.E. (2016). Vitrimers: permanent organic networks with glass-like fluidity. *Chemical Science* 7: 30–38.

66 Brutman, J.P., Delgado, P.A., and Hillmyer, M.A. (2014). Polylactide vitrimers. *ACS Macro Letters* 3: 607–610.

67 Denissen, W., Rivero, G., Nicolaÿ, R. et al. (2015). Vinylogous urethane vitrimers. *Advanced Functional Materials* 25: 2451–2457.

68 Meng, F., Saed, M.O., and Terentjev, E.M. (2019). Elasticity and relaxation in full and partial vitrimer networks. *Macromolecules* 52 (19): 7423–7429.

69 Meng, F., Saed, M.O., and Terentjev, E.M. (2022). Rheology of vitrimers. *Nature Communications* 13: 5753.

70 Meng, F. and Terentjev, E.M. (2018). Fluidization of transient filament networks. *Macromolecules* 51 (12): 4660–4669.

71 Mai, Y.-W. and Yu, Z.-Z. (2006). *Polymer Nanocomposites*. Woodhead Publishing.

72 Hubbe, M.A., Rojas, O.J., Lucia, L.A., and Sain, M. (2008). Cellulosic nanocomposites: a review. *BioResources* 3: 929–980.

73 Zrinyi, M., Barsi, L., and Büki, A. (1997). Ferrogel: a new magneto-controlled elastic medium. *Polymer Gels and Networks* 5: 415–427.

74 Awasthi, S. (2021). A review on hydrogels and ferrogels for biomedical applications. *JOM* 73: 2440–2451.

75 Junot, G., Wei, X., Ortín, J. et al. (2022). Elastically-mediated collective organisation of magnetic microparticles. *Soft Matter* 18: 5171–5176.

76 Shahinpoor, M., Bar-Cohen, Y., Simpson, J.O., and Smith, J. (1998). Ionic polymer-metal composites (IPMCs) as biomimetic sensors, actuators and artificial muscles-a review. *Smart Materials and Structures* 7: R15.

77 Bahramzadeh, Y. and Shahinpoor, M. (2014). A review of ionic polymeric soft actuators and sensors. *Soft Robotics* 1: 38–52.

78 Prost, J., Jülicher, F., and Joanny, J.-F. (2015). Active gel physics. *Nature Physics* 11: 111–117.

79 Style, R.W., Sai, T., Fanelli, N. et al. (2018). Liquid-liquid phase separation in an elastic network. *Physical Review X* 8: 011028.

80 Wei, X., Zhou, J., Wang, Y., and Meng, F. (2020). Modeling elastically mediated liquid-liquid phase separation. *Physical Review Letters* 125: 268001.

81 Sprakel, J., van der Gucht, J., Cohen Stuart, M.A., and Besseling, N.A.M. (2008). Brownian particles in transient polymer networks. *Physical Review E* 77: 061502.

82 Zhao, J. and Meng, F. (2023). Modelling viscoelasticity and dynamic nematic order of exchangeable liquid crystal elastomers. *Physical Review Letters* 131: 068101.